

Knowledge-guided Identification of Condition-specific Rewiring of Dependencies in Biological Networks

Ye Tian^{1,†}, Bai Zhang^{2,†}, Ie-Ming Shih^{2,3,4}, Robert Clarke^{5,6}, Zhen Zhang², Leena Hilakivi-Clarke^{5,6}, Jianhua Xuan¹, David M. Herrington⁷, Eric P. Hoffman⁸, and Yue Wang^{1,*}

¹Bradley Department of Electrical & Computer Engineering, Virginia Tech, Arlington, VA 22203, USA; Departments of

²Pathology, ³Gynecology/Obstetrics & ⁴Oncology, Johns Hopkins Medical Institutions, Baltimore, MD 21231, USA;

⁵Lombardi Comprehensive Cancer Center and ⁶Department of Oncology, Georgetown University, Washington, DC 20057,

USA; ⁷Department of Medicine-Cardiology, Wake Forest University School of Medicine, Winston-Salem, NC 27157, USA;

⁸Research Center for Genetic Medicine, Children's National Medical Center, Washington, DC 20010, USA

Received on XXXXX; revised on XXXXX; accepted on XXXXX

Associate Editor: XXXXXXX

ABSTRACT

Motivation: Modeling cellular and molecular networks is one of the major goals in systems biology, and is an important tool to investigate various mechanisms that orchestrate the activities of genes and proteins in the cells. Among network modeling tasks, identifying the rewiring of network structure is particularly instrumental in revealing and pinpointing the molecular cause of a disease. Besides data-driven approaches, significant efforts have been made to manually curate molecular networks in cells (e.g., protein-protein interactions, biological pathways), providing rich domain knowledge. Effective incorporation of biological prior knowledge into network learning algorithms can leverage domain knowledge and make data-driven inference more robust and biologically relevant. However, biological prior knowledge is neither context-specific nor error-free, only serving as an aggregated source of partially-validated evidence under diverse experimental conditions. Hence, direct incorporation of imperfect and non-specific prior knowledge in specific problems may undermine the inference performance.

Results: To address this challenge, we formulate the inference of condition-specific network structures that incorporates relevant prior knowledge as a convex optimization problem, and develop an efficient learning algorithm to jointly infer the biological networks as well as their changes. Prior knowledge is coded as a graph where edges represent the known biological relationships among the molecular entities. We propose a sampling scheme to estimate the expected error rate due to “random” knowledge and develop a strategy to manage its impact on our algorithm, fully exploiting the benefit of prior knowledge while remaining robust to the false positive edges in prior knowledge. Conversely, the algorithm can identify novel connections between genes without prior knowledge if there is strong evidence in the data supportive of these connections, enabling new biological knowledge and insights from experimental data. We test the proposed method on simulation data sets and demonstrate the effectiveness of this method. We then apply our method to yeast cell

line data and breast cancer microarray data and obtain biologically plausible results.

Availability: The R software package is available at <http://www.cbil.ece.vt.edu/software.htm>.

1 INTRODUCTION

Identifying the mechanisms that orchestrate the activities of genes and proteins in cells is one of the key goals in systems biology studies. Biological networks are context-specific and dynamic in nature. They continuously evolve to adapt to the changing environment (Consortium, 2011). Under different conditions, different regulatory components and mechanisms are activated. Accordingly, the topology of the underlying biological network changes in response to outside stimuli (Beyer, et al., 2007; Chen, et al., 2008; Shen, et al., 2011). The condition-specific biological networks and their topological changes provide great insights into the underlying biology of how the organisms adapt to different conditions, opening up a new era of understanding and treatment of diseases (Bandyopadhyay, et al., 2010; Barabasi, et al., 2011). With the advances in high-throughput genomic technologies, large amounts of genomic data demand effective computational methods to extract biological knowledge and insights. Therefore, a data-driven learning algorithm for condition-specific biological networks is of great interest.

A great deal of effort has been made to accomplish this goal. Many approaches have been proposed previously to model biological networks using gene expression data (Li, et al.), such as probabilistic Boolean networks (Shmulevich, et al.), state-space models (Rangel, et al.), and probabilistic graphical models (Friedman, 2004; Friedman, et al., 2000). Some recent works began to address the condition-specific network construction problem. Changes in the interdependencies among molecular components lead to deep functional and causal relationships among apparently distinct biological outcomes. Instead of asking “which genes are differentially expressed”, further important question here is “which genes are differentially connected” (Ideker and Krogan, 2012). In (Zhang, et

* To whom correspondence should be addressed.

† These authors contributed equally.

al., 2009), we proposed to identify differential dependency networks between two conditions by testing the significance of changes in local dependencies. (Roy, et al., 2011) extended the condition-specific network learning to multiple conditions. Differential biological network analysis has led to new findings and outperformed conventional differential analysis such as differential expression (Hudson, et al., 2009; Reverter, et al., 2010). These methods utilized data in different strategies but have not made use of the rich domain knowledge.

In parallel, in the past decade, a lot of effort has also been expanded to manually curate molecular interactions in cells, such as protein-protein interactions and biological pathways (Kanehisa and Goto, 2000), which can now be conveniently retrieved from relevant biological databases. These biological databases summarize existing knowledge and experimental evidence from multiple sources under diverse conditions, and attempt to delineate a more detailed picture of the interactome in the cells. Such biological prior knowledge provides rich domain knowledge to the biological network inference problem (Ochs). Compared with computational inference purely based on data, proper incorporation of biological prior knowledge into network learning algorithms can effectively leverage domain knowledge and make the inference more biologically meaningful. However, as biological prior knowledge is usually aggregated from multiple sources and under diverse experimental settings, direct incorporation of prior knowledge in specific problems is prone to errors or may even lead to biased results.

To efficiently utilize prior knowledge in the network inference while remaining robust to the false positive edges in the knowledge, we here propose a biological prior knowledge guided learning framework to infer condition-specific biological network structures and their topological changes under two different conditions. In this paper, we also use graphical models to represent condition-specific biological networks. Two characteristics make graphical models suitable for representing biological networks: (1) the probabilistic nature of graphical models automatically takes into account the noise in the data and intrinsic uncertainties in the models, and (2) the graphical representations of the models naturally visualize the relationships of genes, which can facilitate new insights and motivate new biological hypotheses. A similar formulation is used by (Ahmed and Xing, 2009), where the time evolution of network structures is examined with a fused penalty term to encode relationship between adjacent time points, which is substantially different from our formulation where block-wise separable penalties guarantees a fast closed-form solution to the problem. As pointed out by the authors of (Ahmed and Xing, 2009), assessing the statistical significance of edges and differential changes in high-dimensional networks is an important but unsolved question. In our paper, we propose to determine the model parameters to correspond to the required significance level. The important components that make our work to differ from previous efforts include a flexible framework that achieves efficient while robust incorporation of biological knowledge, and the ability to evaluate the statistical significance of differential edges. Another work (Wang, et al., 2013) incorporates knowledge by adjusting Lasso penalties in learning of a single network.

We formulate the problem of biological network structure learning and topological change detection with prior knowledge as a convex optimization problem with ℓ_1 -penalties, and derive an efficient algorithm to solve the problem. Further, we propose a sam-

pling scheme to estimate the expected error rate induced by incorporating random knowledge, which has a maximum entropy distribution over the edges given the number of edges specified in the knowledge. By controlling this error rate under the worst-case scenario, our method can efficiently utilize prior knowledge in the network inference while remaining robust to the false positive edges in the knowledge. We test the proposed method on simulation data to demonstrate the effectiveness of this method, and the simulation results further corroborate our theoretical analysis. We also apply this approach to study how yeast cells respond to oxidative stress, and how apoptotic pathways differ in human breast tumors that subsequently recur versus those that do not recur.

2 METHODS

2.1 Problem Statement

We represent the condition-specific biological networks as graphs. Here we focus on condition-specific biological network structure and their corresponding structural changes under two conditions. Suppose there are p nodes (genes) in the network of interest, and we denote the vertex set as V . Let $G^{(1)} = (V, E^{(1)})$ and $G^{(2)} = (V, E^{(2)})$ be the two undirected graphs under the two conditions. $G^{(1)}$ and $G^{(2)}$ have the same vertex set V , and condition-specific edge sets $E^{(1)}$ and $E^{(2)}$. $E^{(1)}$ and $E^{(2)}$ are expected to have considerable overlap, with only a small amount of edges being different. Such edge changes are of particular interest, since such rewiring may reveal pivotal information on how the organisms respond to different conditions. We use graph $G = (V, E)$ to represent the composite network of graphs $G^{(1)}$ and $G^{(2)}$ under the two conditions. Edges in E are common edges and unique edges under each conditions. We use a combined asymmetric adjacency matrix to represent G , with the upper triangular matrix indicating the connections in $G^{(1)}$ and lower triangular matrix indicating the connections in $G^{(2)}$.

Biological prior knowledge is collected from biological databases such as KEGG pathway database and Human Protein Reference Database. We denote the biological prior knowledge as a knowledge graph $G_w = (V, E_w)$, where the vertex set V is the same set of nodes (genes) and edge set E_w over V is retrieved from biological databases as supported by the existing knowledge or other experimental evidence. G_w is designed to be a directed graph as in some situations direction matters, e.g., transcription-factor and its targets.

We use matrix $\mathbf{W} \in \mathcal{R}^{p \times p}$ to represent the prior knowledge, which is the adjacency matrix of G_w . The elements of \mathbf{W} are either 1 or 0, with $W_{ij} = 1$ indicating the existence of an edge from the j^{th} gene to the i^{th} gene (or their gene products) in the databases, where $i, j = 1, 2, \dots, p, i \neq j$. If the prior knowledge is not directed, every edge is bi-directional and the prior knowledge adjacency matrix \mathbf{W} is symmetric.

The main task in this paper is to infer from data and prior knowledge G_w the condition-specific edge sets E , corresponding to $E^{(1)}$ and $E^{(2)}$. The method is illustrated in Figure 1. Taking condition-specific data and prior knowledge as input, our method infers condition-specific networks with black edges indicating common edges while red and green edges indicating differential edges specific to conditions. Through the method sections we will explain that the novel knowledge incorporation strategy achieves both effectiveness and robustness.

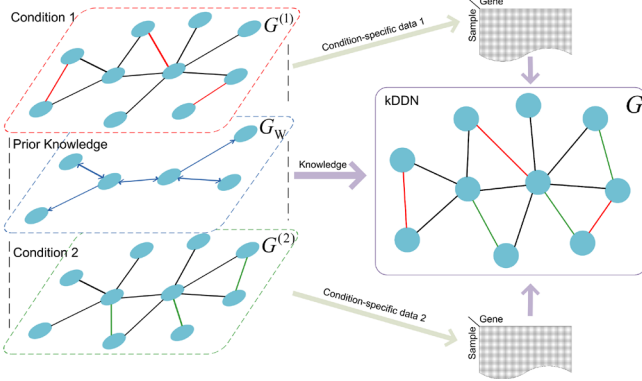


Figure 1. Knowledge-guided differential network learning. Algorithm takes condition-specific data and prior knowledge as input and infers condition-specific networks. Black edges are common edges. Red and green edges are differential edges specific to conditions.

2.2 Convex Optimization Formulation

To take advantage of the prior knowledge in the structural learning and avoid the potential bias introduced by knowledge, we formulate the problem into a convex optimization problem with sparsity constraints, and set the proper weights to achieve both the effectiveness of utilizing the domain knowledge and the robustness to the false positives in the knowledge.

We consider the p nodes in V as p random variables, and denote them as X_1, X_2, \dots, X_p . Suppose there are N_1 samples under condition 1 and N_2 samples under condition 2. Without loss of generality, we assume $N_1 = N_2 = N$. Under the first condition, for variable X_i , we have observations $\mathbf{x}_i^{(1)} = [x_{i1}^{(1)}, x_{i2}^{(1)}, \dots, x_{iN}^{(1)}]^T$, $i = 1, 2, \dots, p$, while under the second condition, we have $\mathbf{x}_i^{(2)} = [x_{i1}^{(2)}, x_{i2}^{(2)}, \dots, x_{iN}^{(2)}]^T$, $i = 1, 2, \dots, p$. Further, let $\mathbf{X}^{(1)} = [\mathbf{x}_1^{(1)}, \mathbf{x}_2^{(1)}, \dots, \mathbf{x}_p^{(1)}]$ be the data matrix under condition 1 and $\mathbf{X}^{(2)} = [\mathbf{x}_1^{(2)}, \mathbf{x}_2^{(2)}, \dots, \mathbf{x}_p^{(2)}]$ be the data matrix under condition 2.

Denote

$$\mathbf{y}_i = \begin{bmatrix} \mathbf{x}_i^{(1)} \\ \mathbf{x}_i^{(2)} \end{bmatrix}, \quad \mathbf{X} = \begin{bmatrix} \mathbf{X}^{(1)} & \mathbf{0} \\ \mathbf{0} & \mathbf{X}^{(2)} \end{bmatrix}, \quad (1)$$

and

$$\boldsymbol{\beta}_i = \begin{bmatrix} \boldsymbol{\beta}_i^{(1)} \\ \boldsymbol{\beta}_i^{(2)} \end{bmatrix} = [\beta_{i1}^{(1)}, \beta_{i2}^{(1)}, \dots, \beta_{pi}^{(1)}, \beta_{i1}^{(2)}, \beta_{i2}^{(2)}, \dots, \beta_{pi}^{(2)}]^T. \quad (2)$$

We formulate the problem of learning structural changes between two conditions as a convex optimization problem, where network structures under two conditions and their changes are simultaneously obtained by solving the optimization problem for each node (variable) X_i , $i = 1, 2, \dots, p$, with the objective function

$$f(\boldsymbol{\beta}_i) = \frac{1}{2} \|\mathbf{y}_i - \mathbf{X}\boldsymbol{\beta}_i\|_2^2 + \lambda_1 \sum_{j=1}^p (1 - W_{ji}\theta) (|\beta_{ji}^{(1)}| + |\beta_{ji}^{(2)}|) + \lambda_2 \|\boldsymbol{\beta}_i^{(1)} - \boldsymbol{\beta}_i^{(2)}\|_1. \quad (3)$$

The solution is obtained by minimizing (3),

$$\begin{aligned} \boldsymbol{\beta}_i &= \arg \min_{\boldsymbol{\beta}_i} f(\boldsymbol{\beta}_i) \\ &= \arg \min_{\boldsymbol{\beta}_i^{(1)}, \boldsymbol{\beta}_i^{(2)}} \frac{1}{2} \|\mathbf{y}_i - \mathbf{X}\boldsymbol{\beta}_i\|_2^2 \\ &\quad + \lambda_1 \sum_{j=1}^p (1 - W_{ji}\theta) (|\beta_{ji}^{(1)}| + |\beta_{ji}^{(2)}|) + \lambda_2 \|\boldsymbol{\beta}_i^{(1)} - \boldsymbol{\beta}_i^{(2)}\|_1 \\ &\text{s.t. } \beta_{ii}^{(1)} = 0, \beta_{ii}^{(2)} = 0. \end{aligned} \quad (4)$$

In (4), the structures of the graphical model under two conditions are learned jointly. The first weighted ℓ_1 -regularization term leads to the identification of sparse graph structure. The second ℓ_1 -regularization term, $\lambda_2 \|\boldsymbol{\beta}_i^{(1)} - \boldsymbol{\beta}_i^{(2)}\|_1$, encourages sparse changes in the model structure and parameters between two conditions, and thereby suppresses the structural and parametric inconsistencies due to noise in the data and limited samples.

The problem (4) can be solved efficiently by the block coordinate descent algorithm. We repeat this procedure to each node X_i , $i = 1, 2, \dots, p$. The non-zero elements of $\boldsymbol{\beta}_i^{(1)}$ indicate the neighbors of the i^{th} node under the first condition and the non-zero elements of $\boldsymbol{\beta}_i^{(2)}$ indicate the neighbors of the i^{th} node under the second condition. Further, as derived in Supplementary Information and shown in supplementary Table S1, “positive” and “negative” connections can be determined by the signs of non-zero elements of the estimated $\boldsymbol{\beta}_i$ corresponding to the differential edges.

2.3 Prior Knowledge Incorporation

The prior knowledge is explicitly incorporated into the formulation by W_{ji} and θ in the weighted ℓ_1 -regularization term,

$\lambda_1 \sum_{j=1}^p (1 - W_{ji}\theta) (|\beta_{ji}^{(1)}| + |\beta_{ji}^{(2)}|)$. The non-zero elements in \mathbf{W} introduce knowledge to the objective function (3). θ is a ℓ_1 penalty relaxation parameter taking value in $[0, 1]$, which works with \mathbf{W} to reduce the penalties on the edges with supporting evidence in the prior knowledge while having no effects on edges with no knowledge.

θ determines to what degree the knowledge will affect the inference. Let us consider two extreme cases: when $\theta = 0$, the algorithm ignores all knowledge information and infers the network structures solely based on data, which is equivalent to the algorithm in (Zhang and Wang, 2010); on the other hand, when $\theta = 1$, the edge between X_j and X_i will always be included if such an edge exists in the prior knowledge, which implies the prior knowledge will have a determining effect on the network inference. Therefore the prior knowledge incorporation needs to find a proper balance between the experimental data and prior knowledge. A proper θ will reduce the penalty applied to $\beta_{ji}^{(c)}$ corresponding to the connection between X_j and X_i with existing prior knowledge. As a result, the connection between X_j and X_i will more likely be detected.

From a Bayesian perspective, as pointed out in (Tibshirani, 1996), the ℓ_1 penalty term $\|\boldsymbol{\beta}_i^{(c)}\|_1$ is equivalent to independent Laplace priors for the $\beta_{ji}^{(c)}$, $j = 1, 2, \dots, p$, $c = 1, 2$, which follow

$$\text{pdf}(\beta_{ji}^{(c)}) = \frac{1}{2b} \exp\left(-\frac{|\beta_{ji}^{(c)}|}{b}\right) \quad (5)$$

where $b = 1/(\lambda_1(1 - W_{ji}\theta))$. When prior knowledge supports the edge between node i and node j , a non-zero θ adjusts the prior distribution for this edge ($\beta_{ji}^{(c)}$) with a larger b , making it more likely to be detected.

We want to effectively incorporate the true information in the prior knowledge, while limiting the adverse effects caused by the spurious edges. Here we choose a strategy to control such adverse effects incurred in the worst-case scenario under which the given prior knowledge is totally random. In this case, the entropy of the knowledge distribution over the edges

is maximized and the information introduced to the inference is minimal. Incorporating such random knowledge, the inference results will deviate from the purely data driven result. Then, θ is carefully chosen so that the expected deviation is controlled within acceptable range in the worst-case scenario, which guarantees the robustness when the prior knowledge is highly inconsistent with the underlying ground-truth.

We use Hamming distance between two adjacency matrices as a measurement for the dissimilarity of two graphs. Let $G_T = (V, E_T)$ denote the ground-truth graph with edge set E_T , $G_X = (V, E_X)$ denote the graph learned purely from data, *i.e.* $\mathbf{W} = \mathbf{0}$, and $G_{X, \mathbf{W}_R, \theta} = (V, E_{X, \mathbf{W}_R, \theta})$ denote the graph learned with prior knowledge. \mathbf{W}_R indicates that the prior knowledge is ‘‘random’’. Let $d(G_*, G_*)$ denote the Hamming distance between two graphs. Further, let $|E_*|$ be the number of edges in the graph G_* .

The inference error rate associated with the purely data result G_X is $d(G_T, G_X)/|E_T|$, which is an unknown baseline when determining the degree of knowledge incorporation θ . Even if the prior knowledge is the worst case, a proper θ is expected to control the increase in the error rate within an acceptable range.

Since G_T is unknown, we instead control the increase in the error rate indirectly by evaluating the effect of random knowledge against G_X , the purely data-driven inference result. To be more specific, we use a sampling-based algorithm to find the empirical distribution of $d(G_X, G_{X, \mathbf{W}_R, \theta})$, and choose the largest $\theta \in [0, 1]$ that satisfies:

$$\begin{aligned} \hat{\theta} &= \max \theta \\ \text{s.t. } & \mathbb{E}[d(G_X, G_{X, \mathbf{W}_R, \theta})/|E_X|] \leq \delta. \end{aligned} \quad (6)$$

It is important to note that our strategy for determining θ is similar to (in spirit) the one used in Neyman-Pearson hypothesis testing, that is, incorporation of prior knowledge is maximized while subject to the worst-case error rate below a user-desired bound δ .

A natural question is whether using G_X instead of G_T to control the increase in the error rate induced by random knowledge is legitimate. To answer this question, we show in Theorem 1 (proof included in Supplementary Information) that the θ obtained in (6) in fact controls an upper bound of $\mathbb{E}[d(G_T, G_{X, \mathbf{W}_R, \theta})/|E_T|]$, *i.e.* the increase in the network inference error rate induced by random prior knowledge (the worst-case scenario), under the assumption that the number of false negatives (*FN*) in data-driven result G_X is smaller than the number of false positives (*FP*). As we adopt a strategy to refrain from falsely joining unconnected edges (Meinshausen and Bühlmann, 2006), this assumption is generally held. This approach is illustrated in Figure 2.

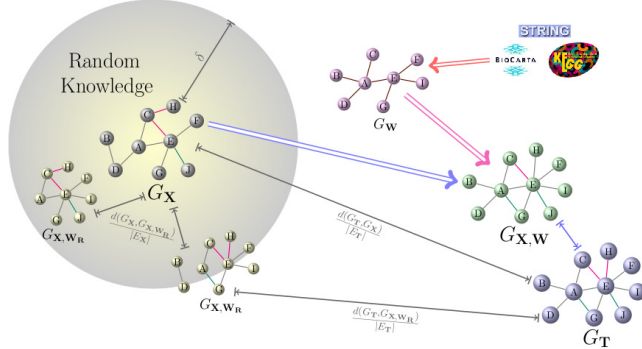


Figure 2. Illustration of Theorem 1. Networks are represented by connected clusters of nodes, with gray edges indicating common connections under both conditions, green and red edges indicating condition-specific connections. G_T is the underlying ground-truth. G_X is the purely data result. δ controls the increase in the error rate induced by random knowledge within

the shaded region. By incorporating prior knowledge with good quality, the learning result $G_{X, \mathbf{W}}$ can be significantly improved.

Theorem 1. For a given $\delta \in [0, 1]$, if the prior knowledge incorporation parameter θ satisfies the inequality

$$\frac{\mathbb{E}[d(G_X, G_{X, \mathbf{W}_R, \theta})]}{|E_X|} \leq \delta, \quad (7)$$

then the increase in the error rate induced by incorporating random prior knowledge is bounded by δ , more specifically,

$$\frac{\mathbb{E}[d(G_T, G_{X, \mathbf{W}_R, \theta})]}{|E_T|} \leq \frac{d(G_T, G_X)}{|E_T|} + \delta. \quad (8)$$

2.4 Block Coordinate Descent Algorithm

Although the optimization problems with ℓ_1 -regularization can be solved readily by existing convex optimization techniques, a lot of efforts have been made to solve the problems efficiently by exploiting the special structures of the problems. Coordinate-wise descent algorithms have been studied in Lasso related problems, such as Lasso, garotte, and elastic net (Friedman, et al., 2007). It is shown in (Friedman, et al., 2008) that a coordinate descent procedure for Lasso, graphical Lasso, is 30-4000 times faster than competing methods, making it computationally attractive. We propose a block coordinate descent algorithm to solve the optimization problem in (4), and derive the corresponding closed-form solution for the sub-problem.

We adopt the coordinate descent idea since in our formulation the penalty term $\lambda_1 \sum_{j=1}^p (1 - W_{ji} \theta) (|\beta_{ji}^{(1)}| + |\beta_{ji}^{(2)}|) + \lambda_2 \|\beta_i^{(1)} - \beta_i^{(2)}\|_1$ has block-wise separability (Tseng, 2001). For each node X_i , $i = 1, 2, \dots, p$, the objective function (3) can be rewritten as

$$f(\beta_i) = \frac{1}{2} \|y_i - X \beta_i\|_2^2 + \lambda_1 \sum_{j=1}^p (1 - W_{ji} \theta) (|\beta_{ji}^{(1)}| + |\beta_{ji}^{(2)}|) + \lambda_2 \sum_{j=1}^p (|\beta_{ji}^{(1)} - \beta_{ji}^{(2)}|) \quad (9)$$

The non-differentiable part of $f(\beta_i)$ can be written as the sum of p terms with non-overlapping members, $(\beta_{ji}^{(1)}, \beta_{ji}^{(2)})$, $j = 1, 2, \dots, p$. Each $(\beta_{ji}^{(1)}, \beta_{ji}^{(2)})$, $j = 1, 2, \dots, p$, is a coordinate block.

The essence of the block coordinate descent algorithm is ‘‘one-block-at-a-time’’. At iteration $r + 1$, only one coordinate block, $(\beta_{ji}^{(1)}, \beta_{ji}^{(2)})$, is updated, with the remaining $(\beta_{li}^{(1)}, \beta_{li}^{(2)})$, $l \neq j$, fixed at their values at iteration r . Given

$$\beta_i^r = [\beta_{1i}^{(1),r}, \beta_{2i}^{(1),r}, \dots, \beta_{pi}^{(1),r}, \beta_{1i}^{(2),r}, \beta_{2i}^{(2),r}, \dots, \beta_{pi}^{(2),r}]^T, \quad (10)$$

at iteration $r + 1$, the estimation is updated according to the following sub-problem

$$\begin{aligned} \beta_i^{r+1} &= \arg \min_{\beta_i} f(\beta_i) \\ \text{s.t. } & \beta_{li}^{(1)} = \beta_{li}^{(1),r}, \beta_{li}^{(2)} = \beta_{li}^{(2),r}, \text{ for } l = 1, 2, \dots, p, l \neq j. \end{aligned} \quad (11)$$

We use a cyclic rule to solve the sub-problem and update parameter estimation iteratively, *i.e.*, update parameter pair $(\beta_{ji}^{(1)}, \beta_{ji}^{(2)})$ at iteration $r+1$, and $j = ((r+1) \bmod p) + 1$. The closed-form solution to the sub-problem is derived in Supplementary Information.

We summarize the block coordinate descent optimization procedure to solve problem (4) in Algorithm S1. The convergence of the algorithm is guaranteed by Theorem 4.1 proposed by (Tseng, 2001).

2.5 Degree of Prior Knowledge Incorporation

We want to select a proper θ that efficiently utilizes the information in the prior knowledge while remaining robust to the spurious edges in the

knowledge. We estimate the expected normalized deviation under random knowledge by a sampling algorithm, and solve (6) subsequently.

Given the number of edges specified in the prior knowledge, M , $M = 0, \dots, \binom{p}{2}$, we randomly sample M edges from all possible edges formed by pairs of vertex in V as “random” prior knowledge to form a \mathbf{W}_R , and solve the optimization problem (4) to learn the condition-specific network with prior knowledge. The deviation of the network with prior knowledge from the network inferred purely based on data is calculated. By repeating this process B times (B is set to 1000 in this paper), we can obtain the empirical distribution of this deviation. Based on this empirical distribution, we utilize its average as the estimate of the expected increase of error rate. We use binary search to find the θ as the solution of problem (6) efficiently.

We summarize the steps above in Algorithm S2 in Supplementary Information. This procedure is computationally intensive, and therefore the computational efficiency of Algorithm S1 becomes indispensable in the development of this approach.

2.6 Choice of Penalty Parameters and Significance Assessment of Differential Edges

As we discussed previously, the first ℓ_1 -regularization term, $\lambda_1 \sum_{j=1}^p (1 - W_{ji} \theta) (|\beta_{ji}^{(1)}| + |\beta_{ji}^{(2)}|)$, leads to the identification of sparse graph structures, and the second ℓ_1 -regularization term, $\lambda_2 \|\beta_i^{(1)} - \beta_i^{(2)}\|_1$, suppresses the inconsistencies of the network structures and parameters between two conditions.

For the first penalty term λ_1 , we consider the case without prior knowledge $\mathbf{W} = \mathbf{0}$ and $\lambda_2 = 0$. In this case, the problem (4) is equivalent to applying Lasso under two conditions separately and the structures of two networks are learned without considering statistical differences between them. The λ_1 controls the sparsity of the learned graph, and the Algorithm S1 is reduced to a coordinate descent algorithm, in which each sub-problem is Lasso with two orthogonal predictors. Under Gaussian assumption, according to Theorem 3 in (Meinshausen and Bühlmann, 2006), the value of λ_1 determined by confining the probability of falsely claiming an edge between two distinct neighborhood no larger than α_1 (which is typically set to 0.05),

$$\lambda_1 = \frac{2}{n} \left(1 - \Phi \left(\frac{\alpha_1}{2pn^2} \right) \right) \quad (12)$$

in which n is the sample size N .

The second parameter λ_2 controls the sparsity of structural and parametric changes between two conditions. At a given significance level α_2 , (e.g., $\alpha_2 = 0.05$ is used in this paper), only differential edges that are statistically significant rather than random will have differential edge properties. The λ_2 corresponding to α_2 is found by putting the type I error rate under null distribution in the vicinity of α_2 using batches of permuted samples. Under the null distribution, there is no change between two networks. Suppose the size of the network or the number of edges in the network is E under null distribution, the expected type I error rate should be α_2 , i.e., there are still $\alpha_2 E$ edges are falsely claimed as differential edges. λ_2 is then found by gradually increasing it from 0 until type I error rate falls into the vicinity of α_2 under null distribution to guarantee desired detection power.

After determining the λ_2 and learning the differential network, we further use another permutation test to assess the p -value of differential edges e_{ij} . In B times permutation, we count how many times that the edge between i and j are claimed as differential, and divide it by B to get the p -value of differential edge e_{ij} .

3 RESULTS

We demonstrated the utility of the proposed approach by using both simulation data and real biological data. In the simulation study, we created networks with different sizes and compared with peer methods how this knowledge incorporation scheme effectively recover overall network structure, identify differential networks and tolerate false positives in the prior knowledge. In real data applications, we first learned the network rewiring of the cell cycle pathway of the budding yeast in response to oxidative stress, and then applied the method to study the different apoptotic signaling between recurring and non-recurring breast cancer tumors. An application to study muscular dystrophy is included in Supplementary Information. For convenience, we abbreviate the name of our method as kDDN.

3.1 Simulation Shows Effectiveness and Designed Features of Knowledge Guided Learning

We constructed a Gaussian Markov random field with $p = 100$ nodes and 150 samples following the approach used in (Meinshausen and Bühlmann, 2006), and then randomly modified 10% of the edges to create two condition-specific networks with sparse changes. The details of simulation data generation procedure are provided in Supplementary Information. The number of edges in prior knowledge M was set to be the number of common edges in the two condition-specific networks, and δ was set to 0.1.

To assess the effectiveness of prior knowledge incorporation and robustness of kDDN when false positive edges were present in prior knowledge, we examined the network inference precision and recall of overall network and differential network as the false positive rate in the prior knowledge increases. Overall network performance puts two condition-specific networks together to measure how well the method recovers network structures. Differential network only includes edges specific to either condition.

It is important to note that both false positives and false negatives in the prior knowledge here are with respect to the condition-specific ground truth from which the data are generated. Thus, false positives in prior knowledge may contribute more learning errors, false negatives will not (theoretically) worsen network learning performance.

Starting from prior knowledge without any false positive edges, we gradually increased the false positive rate in prior knowledge until all prior knowledge was false. At each given false positive rate in the prior knowledge, we randomly created 1,000 sets of prior knowledge, and compared the performance of kDDN on each of the network with two baselines: (1) a purely data-driven result without incorporating knowledge; and (2) a naïve baseline of knowledge incorporation by directly superimposing the prior knowledge network upon the purely data result.

We measure the precision and recall of the inference results as the false positive rate in the prior knowledge increases, as shown in Figure 3(a) and Figure 3(b). The brown circles indicate the purely data performance without prior knowledge, which are not affected by the false positive rate in the prior knowledge; the blue squares indicate the average precision or recall of network inference with kDDN at different false positive rates in the prior knowledge; the red diamond indicate the performance of the naïve baseline; and

the box plot shows the 5th, 25th, 75th and 95th percentile of the performance at each false positive rate in prior knowledge.

Precision measures the fraction of edges in the learned network that are consistent with the ground-truth. It reflects the robustness to the false positive edges and efficiency of utilizing the information in prior knowledge. Figure 3(a) shows that, as expected, the false positive rate in prior knowledge has limited effect on the precision of kDDN. With more false positives in the prior knowledge, the precision decreases but is still around the purely data baseline and much better than the naïve baseline. While the naïve baseline suffers significantly from the false positives in prior knowledge as it indiscriminately accepts all edges in prior knowledge without considering evidence in the data. This observation corroborates the design of our method: to control the false detection incurred by the false positives in the prior knowledge. At the point where the false positive rate in the prior knowledge is 100%, the decrease of precision compared with the purely data based result is bounded within δ .

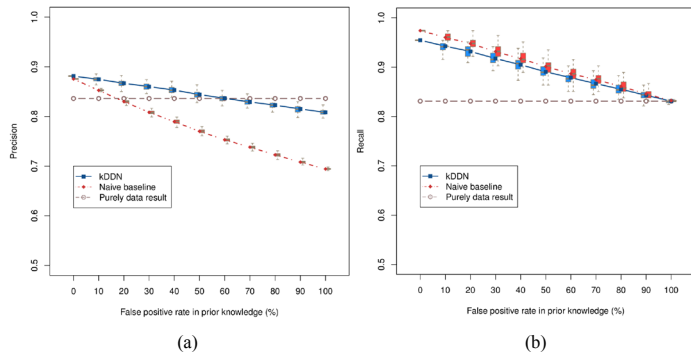


Figure 3. The effects of false positive rate in the prior knowledge on inference precision and recall of overall network.

Recall measures the fraction of ground-truth edges that are successfully detected. It reflects the ability of prior knowledge in helping recover missing edges. Figure 3(b) shows that the recall decreases as the false positive rate in prior knowledge increases for both the kDDN and the naïve baseline. When the prior knowledge is 100% false, the recall is the same with that of the purely data based result, because in this case the prior knowledge brings in no additional information and the inference result does not change. When the true positive edges are included in the prior knowledge, the recall becomes higher than that of the purely data based result because more edges are correctly detected by harnessing the correct information in the prior knowledge. The naïve baseline is slightly higher in recall since it calls an edge as long as knowledge contains it, while kDDN calls an edge only when both knowledge and data evidence are present. But the closeness between kDDN and naïve baseline demonstrates the high efficiency of our method in utilizing the true information in prior knowledge.

We then evaluate the effect of knowledge incorporation solely on the identification of differential network following the same protocol. The results are shown in Figure 4.

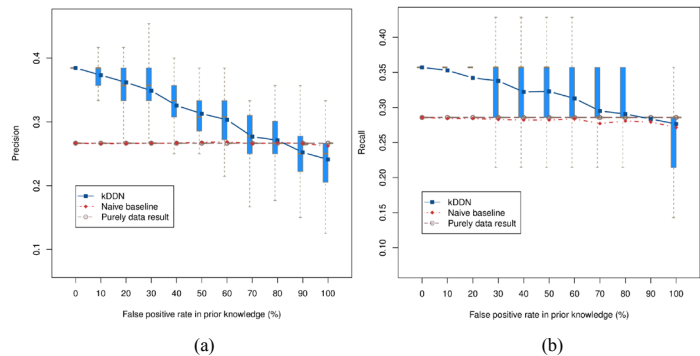


Figure 4. The effects of false positive rate in the prior knowledge on inference precision and recall of differential network.

For differential network recovery, naïve baseline is almost identical to purely data results as the prior knowledge seldom includes a differential edge in a large network with sparse changes. While similar advantages of kDDN apply. Our method has better precision and recall, and bounds the performance degradation when knowledge is totally wrong. Unlike the naïve baseline where knowledge is irrelevant to data, we model the inference with knowledge and data together, so knowledge is able to help identify differential edges as well.

Depending on specific conditions, false positives in prior knowledge may not distribute uniformly, but tend to aggregate more towards certain nodes. Experiments with biased knowledge shown in supplementary Figures S5-S8 indicate no difference or little improvement against random knowledge, confirming that random knowledge represents the worst case and the bound according to random knowledge is sufficient.

Under noise cases with different signal to noise ratios, the approach still works as desired and the experiment results are included in the supplementary Figures S2-S4. False negatives in prior knowledge do not affect the inference as they are not involved in the formulation. We demonstrated this point with experiments shown in supplementary Figures S9 and S10 by increasing the amount of false negatives in prior knowledge. At the extreme case, prior knowledge only contains false negatives and the inference regresses to purely data results.

3.2 Empirical type I error rate for simulated data sets under the null hypothesis

To the best of our knowledge, our method is the first to assess the significance of differential edges. To assess if our method identifies the differential edges at the right significance level, we test the type I error rate of differential edge detection using multiple simulation data sets under the null distribution (no differential edges between the two networks). If the type I error rate is either too conservative or too liberal, the p -value fails to reflect the actual false positive rate and we cannot control how many false positives are detected by setting a p -value based threshold (Chen, et al., 2011). Null data sets based on multivariate Gaussian distribution are simulated and the false positive rate when $\alpha = 0.05$ are calculated with networks of size 80, 100, 120 and 150 in number of nodes. Experiments show the average type I error rate under null converge exactly to α and the standard deviation decreases with

larger network size (Figure S11). This accuracy in p -value estimation gives stronger confidence in differential edge detection.

3.3 Performance comparisons

We compared our joint learning method kDDN with four peer methods: 1) DDN (independent learning) (Zhang, et al., 2009), 2) csLearner (joint learning) (Roy, et al., 2011), 3) Meinshausen’s method (independent learning) (Meinshausen and Bühlmann, 2006), and 4) Tesla (joint learning) (Ahmed and Xing, 2009). csLearner can learn more than two networks but we restricted the condition to two. Meinshausen’s method learns the network under single condition, and we combined the results learned under each condition to get conserved network and differential network. Tesla learns a time-evolving network, but can be adapted to two-condition learning as well. Only kDDN can assign edge-specific p -values to differential edges. Please note although kDDN and DDN look consistent in names, they are substantially different methods.

Parameters in kDDN are automatically inferred from data as described in Section 2.6. We set DDN to detect pair-wise dependencies as it turns out to be the most accurate in the experiment. The number of neighbors in csLearner is set to “4” (the ground truth value). Meinshausen’s method uses the same λ_1 as inferred by kDDN as it is a special case of kDDN under one condition without prior knowledge. Tesla uses the empirically-determined optimum parameter values since the parameter selection was not automatic but relies on user input. These algorithmic parameter settings should favor the peer methods in the comparisons.

To assess the impact of prior knowledge in learning the networks, we run kDDN under three scenarios: data-only (kDDN.dt), data plus true prior knowledge (kDDN.tk), and data plus “random” prior knowledge (kDDN.fk).

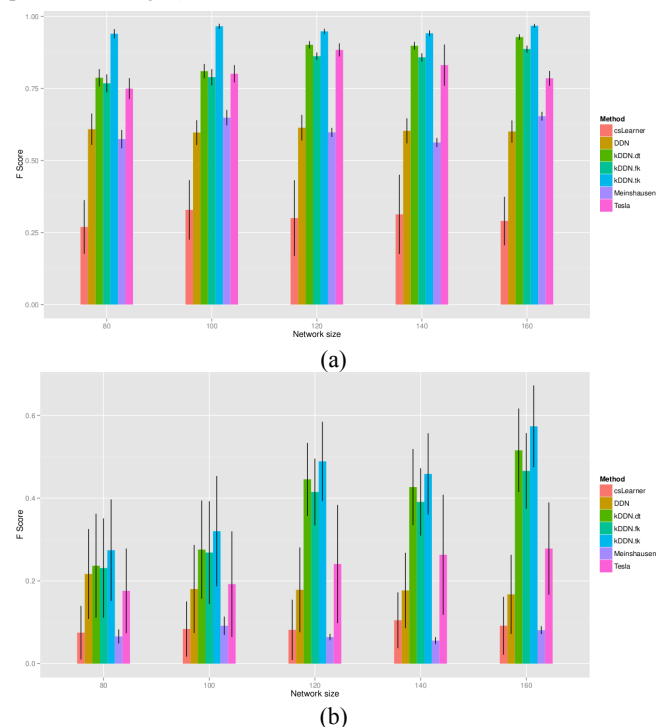


Figure 5. Performance comparison. (a) Recovery of overall network. (b) Recovery of differential network.

The ground truth networks consist of 80, 100, 120, 140 and 160 nodes, and correspondingly with 120, 150, 200, 200 and 240 samples. For each network size, 100 simulation datasets are generated. We evaluate the performance of inferring both overall and differential edges of the underlying networks using the F-score (harmonic mean of precision and recall, $2 \frac{\text{precision} * \text{recall}}{\text{precision} + \text{recall}}$) and precision-recall averaged over all datasets under each network size.

Figure 5(a) compares the ability of recovering overall networks. We see kDDN.tk consistently outperforms all peer methods, and kDDN.dt and kDDN.fk performs comparatively to Tesla (best-performed peer method). Independent learning methods, DDN and Meinshausen’s method, place third due to its incapability of jointly using data.

Figure 5(b) shows the comparison of performance on recovering differential edges. Results show that kDDN consistently outperforms all peer methods under all scenarios. The fact that kDDN determines λ_2 according to the statistical significance of differential edges helps kDDN performs better in differential edge detection than Tesla. It is also clear that single-condition method is not able to find the differential edges correctly and performs the worst.

In supplementary Figures S12 and S13, performance of methods are displayed on the plane of precision-recall, with background heatmap indicating F score ranging from 0 to 1. Again, we can reach the same conclusions by evaluating precision and recall.

Through these comparisons, we show that single-condition and/or independent learning is less effective than joint learning, and kDDN achieves better performance than peer methods. High-quality knowledge further improves kDDN performance, while kDDN is robust enough to even totally random prior knowledge.

3.4 Pathway Rewiring in Yeast Uncovers Cell Cycle Response to Oxidative Stress

To test the utility of the methods in real biological study, we applied it to a public data set GSE7645. This data set used budding yeast *Saccharomyces cerevisiae* to study the genome-wide response to oxidative stress imposed by cumene hydroperoxide (CHP). Yeast cultures were grown in controlled batch conditions, in 1 L fermentors. Three replicate cultures in mid-exponential phase were exposed to 0.19 mM CHP, while three non-treated cultures were used as controls. Samples were collected at $t=0$ (immediately before adding CHP) and at 3,6,12,20,40,70 and 120 min after adding the oxidant. Samples were processed for RNA extraction and profiled using Affymetrix Yeast Genome S98 arrays.

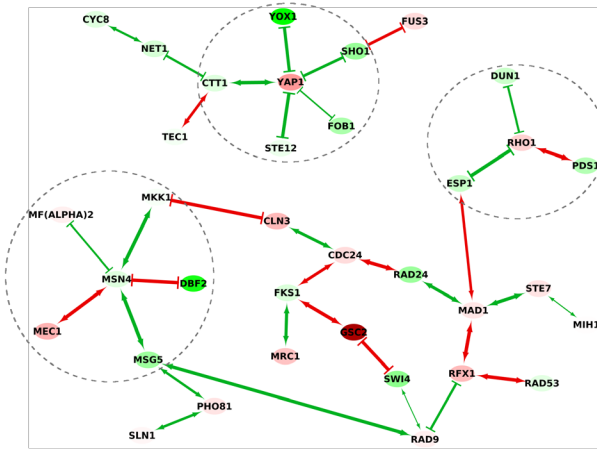


Figure 6. Differential dependency network in budding yeast reflects the cell cycle response to oxidative stress.

We analyzed the network changes of cell cycle related genes with structural information from KEGG yeast pathway as prior knowledge. We added a well studied yeast oxidative stress response gene *Yap1* (Costa, et al., 2002; Ikner and Shiozaki, 2005; Jamieson, 1998; Kuge, et al., 1997) to the knowledge network and related connections gathered from Saccharomyces Genome Database (Cherry, et al., 2011). The learned differential network result is shown in Figure 5, in which nodes represent genes involved in the pathway rewiring, and edges show the condition-specific connections. Red edges are connections in control and green edges are connections under stress. Edges with arrow heads and tails indicate positive connections while edges with bar heads and tails indicate negative connections. Wider edges have higher significance.

Oxidative stress is a harmful condition in a cell, tissue, or organ, caused by an imbalance between reactive oxygen species and other oxidants and the capacity of antioxidant defense systems to remove them. It is clear from the result that *Yap1*, *Rho1* and *Msn4* are at the center of the network response to oxidative stress. They are activated under oxidative stress and many connections surrounding them are created (green edges). *Yap1* is a major transcription factor that responds to oxidative stress (Costa, et al., 2002; Ikner and Shiozaki, 2005; Jamieson, 1998; Kuge, et al., 1997). *Msn4* is considered as a general responder to environmental stresses including heat shocks, hydrogen peroxide, hyper-osmotic shock, amino acid starvation (Causton, et al., 2001; Gasch, et al., 2000). *Rho1* is known to resist the oxidative damage and facilitate cell survival (Lee, et al., 2011; Petkova, et al., 2010; Singh, 2008). The involvement of these central genes captured the dynamic response of how yeast cell sense and react to oxidative stress. The edge between *Yap1* and *Ctt1* under stress grants more confidence to the result. *Ctt1* plays a role as antioxidant in the defense to oxidative stress (Grant, et al., 1998), and the coordination between *Yap1* and *Ctt1* in protecting cells from oxidative stress is well established (Lee, et al., 1999). This result depicted the dynamic response of yeast when exposed to oxidative stress and many findings had support from previous studies, which validated the effectiveness of the methods in revealing underlying mechanisms as well as providing potential novel understandings. These insights would be largely missed by conventional differential expression analysis as the important genes *Rho1*, *Msn4*, *Yap1* and *Ctt1* ranks 13, 20, 64 and

84 among all 86 involved genes based on *t*-test *p*-values. In a comparison with data-only results in Supplementary Information, 14 different differential edges are found.

3.5 Apoptosis pathway in early recurrent and non-recurrent breast cancer patient

The network rewiring analysis can be utilized to study the mechanistic differences between long-term outcomes of a disease and help find the underlying key players that cause the differences. For example, 50% of estrogen receptor positive breast cancers recur, but the mechanisms involved in causing the recurrence remain unknown. Understanding of the mechanisms of breast cancer recurrence can provide critical information for early detection and prevention. We used gene expression data from a clinical study (Loi, et al., 2007) to learn the differences in apoptosis pathway in the primary tumors between recurring and non-recurring patients. We compared the pathway changes in tumors obtained from patients whose breast cancer recurred within 5 years after treatment and from patients who remained recurrence free for at least 8 years after treatment. There were 47 and 48 tumor samples in the recurring and non-recurring groups, respectively. Gene expression data were generated using Affymetrix U133A arrays. We used the apoptosis pathway from KEGG as prior knowledge.

Following the same presentation as in the yeast study, red edges are connections established in recurring patients, and green edges are connections unique to non-recurring patients. Differences in the signaling among genes in the apoptosis pathway between tumors in patients that subsequently recurred or remained cancer free are shown in Figure 7.

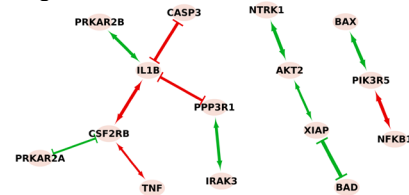


Figure 7. Rewiring of apoptosis pathway in breast cancer patients with/without recurrence. Red edges are connections in recurring patients, and green edges are connections in non-recurring patients.

Three inflammatory/immune response genes (*IL1B*, *NFkB* and *TNFa*) that are all linked to increased resistance to breast cancer treatment were identified in the recurring tumors. These genes formed a path to inhibit proapoptotic *CASP3* and *PPP3R1* (Su, et al., 2012), and to activate pro-survival gene *PIK3R5* or *CSF2RB* that maintains the cell. In contrast, green edges that were present in non-recurring tumors form paths to both anti-apoptotic *XIAP*/*AKT2* pathway and proapoptotic *BAX* and *BAD*.

- Kuge, S., Jones, N. and Nomoto, A. (1997) Regulation of γ AP-1 nuclear localization in response to oxidative stress, *EMBO J*, **16**, 1710-1720.
- Lee, J., et al. (1999) Yap1 and Skn7 Control Two Specialized Oxidative Stress Response Regulons in Yeast, *Journal of Biological Chemistry*, **274**, 16040-16046.
- Lee, M.E., et al. (2011) The Rho1 GTPase Acts Together With a Vacuolar Glutathione S-Conjugate Transporter to Protect Yeast Cells From Oxidative Stress, *Genetics*, **188**, 859-870.
- Li, H., et al. (2008) Inferring regulatory networks., *Frontiers in bioscience : a journal and virtual library*, **13**, 263-275.
- Loi, S., et al. (2007) Definition of Clinically Distinct Molecular Subtypes in Estrogen Receptor-Positive Breast Carcinomas Through Genomic Grade, *Journal of Clinical Oncology*, **25**, 1239-1246.
- Meinshausen, N. and Bühlmann, P. (2006) High-dimensional graphs and variable selection with the Lasso, *The Annals of Statistics*, **34**, 1436-1462.
- Murphy, K., et al. (2000) Bcl-2 inhibits Bax translocation from cytosol to mitochondria during drug-induced apoptosis of human tumor cells, *Cell Death and Differentiation*, **7**, 102-111.
- Ochs, M.F. (2010) Knowledge-based data analysis comes of age, *Brief Bioinform*, **11**, 30-39.
- Petkova, M.I., Pujol-Carrion, N. and de la Torre-Ruiz, M.A. (2010) Signal flow between CWI/TOR and CWI/RAS in budding yeast under conditions of oxidative stress and glucose starvation, *Communicative & Integrative Biology*, **3**, 555-557.
- Rangel, C., et al. (2004) Modeling T-cell activation using gene expression profiling and state-space models, *Bioinformatics*, **20**, 1361-1372.
- Reverter, A., et al. (2010) Regulatory impact factors: unraveling the transcriptional regulation of complex traits from expression data, *Bioinformatics*, **26**, 896-904.
- Roy, S., Werner-Washburne, M. and Lane, T. (2011) A multiple network learning approach to capture system-wide condition-specific responses, *Bioinformatics*, **27**, 1832-1838.
- Shen, C., et al. (2011) A modulated empirical Bayes model for identifying topological and temporal estrogen receptor alpha regulatory networks in breast cancer, *BMC Syst Biol*, **5**, 67.
- Shmulevich, I., et al. (2002) Probabilistic Boolean networks: a rule-based uncertainty model for gene regulatory networks, *Bioinformatics*, **18**, 261-274.
- Singh, K. (2008) Oxidant-Induced Cell Death Mediated By A Rho Gtpase In *Saccharomyces cerevisiae*. Ohio State University.
- Su, Z., et al. (2012) The calcineurin B subunit induces TNF-related apoptosis-inducing ligand (TRAIL) expression via CD11b-NF- κ B pathway in RAW264.7 macrophages, *Biochemical and Biophysical Research Communications*, **417**, 777-783.
- Tibshirani, R. (1996) Regression shrinkage and selection via the lasso, *Journal of the Royal Statistical Society, Series B*, **58**, 267-288.
- Tseng, P. (2001) Convergence of a block coordinate descent method for nondifferentiable minimization, *Journal of Optimization Theory and Applications*, **109**, 475-494.
- Wang, Z., et al. (2013) Incorporating prior knowledge into Gene Network Study, *Bioinformatics*.
- Zhang, B., et al. (2009) Differential Dependency Network Analysis to Identify Condition-Specific Topological Changes in Biological Networks, *Bioinformatics*, **25**, 526-532.
- Zhang, B. and Wang, Y. (2010) Learning Structural Changes of Gaussian Graphical Models In Controlled Experiments. *Conference on Uncertainty in Artificial Intelligence (UAI 2010)*.